Atmospheric
Chemistry
and Physics

Boundary layer nucleation as a source of new CCN in savannah environment

L. Laakso[1,2], J. Merikanto[3], V. Vakkari[3], H. Laakso[3], M. Kulmala[3], M. Molefe[4], N. Kgabi[4], D. Mabaso[5], K. S. Carslaw[6], D. V. Spracklen[6], L. A. Lee[6], C. L. Reddington[6], and V.-M. Kerminen[1,3]

[1]Finnish Meteorological Institute, P.O. Box 64, 00014 Helsinki, Finland
[2]School of Physical and Chemical Sciences, North-West University, Potchefstroom, South Africa
[3]Department of Physical Sciences, University of Helsinki, P.O. Box 64, 00014 Helsinki, Finland
[4]Department of Physics, North-West University, Private Bag X 2046, Mmabatho, South Africa
[5]Rustenburg Local Municipality, Rustenburg, South Africa
[6]School of Earth and Environment, University of Leeds, Leeds, UK

Correspondence to: L. Laakso (lauri.laakso@fmi.fi)

Abstract. The South African savannah region is a complex environment of air pollution and natural emissions influenced by a strong seasonal cycle in biomass burning and strong precipitation. However, the scarcity of long-term observations means that the knowledge of controlling aerosol processes in this environment is limited. Here we use a recent dataset of 18 months of aerosol size distribution observations trying to understand the annual cycle of cloud condensation nuclei (CCN).

Our observations show that the concentration of CCN-sized particles remains, in line with previous studies, high throughout the year with the highest concentrations during the dry winter and the lowest during the wet summer. During the wet season with reduced anthropogenic and biomass burning primary emissions, this pool of CCN is partly filled by boundary layer nucleation with subsequent growth. The enhanced importance of formation and growth during the wet season is addressed to increased biogenic activity together with enhanced free tropospheric removal decreasing the concentration of pre-existing CCN. During the dry season, while frequent new particle formation takes place, particle growth is reduced due to reduced condensing vapour concentrations. Thus in the dry season particles are not able to grow to sizes where they may act as CCN nearly as efficiently as during the wet season.

The observations are compared to simulations by a global aerosol model GLOMAP. To our surprise, the global aerosol model utilized to explain the observations was not capable of re-producing the characteristics of particle formation and the annual CCN cycle, despite earlier good performance in predicting the particle concentrations in a number of diverse environments, including the South African savannah region. While the average yearly CCN concentrations of modelled CCN is close to observed concentrations, the characteristics of nucleation bursts and subsequent growth are not captured satisfactory by the model. Our sensitivity tests using different nucleation parameterizations and condensing organic vapour production rates show that neither of these is likely to explain the differences between observed and modelled nucleation and growth rates.

A sensitivity study varying 28 modelling parameters indicates that the main uncertainties in the result are due to uncertainties in biomass burning emissions during the dry season, and anthropogenic sulphur emissions during the wet season, both in terms or emitted mass and particle sizes. The uncertainties appear to be mostly related to uncertainties in primary particle emissions, including the emissions variability not captured by monthly emission inventories. The results of this paper also highlights the fact that deficiencies in emissions estimates may result in deficiencies in particle production fluxes, while the end product such as modelled CCN concentration may be in line with observations.

1 Introduction

Clouds, especially aerosol-cloud interactions, constitute perhaps the largest source of uncertainty in predicting the behaviour of the Earth's climate system (IPCC, 2007; Jones et al., 2009; Khain, 2009). The influence of aerosols on the reflectivity, lifetime and precipitation patterns of clouds depends principally on the number concentration, chemical composition and mixing state of particles able to act as cloud condensation nuclei (CCN).

Atmospheric CCN originate either from primary particle emissions or from new-particle formation. In both cases, CCN number concentrations are affected by various aerosol transformation processes taking place in the atmosphere (Andreae and Rosenfeld, 2008).

In southern Africa, the characteristics of CCN have been studied in two field campaigns, SAFARI 2000 and ARREX (Ross et al., 2003). One of the main findings of these studies was that CCN concentrations during the wet season were comparable to or even higher than those during the dry season. This is surprising, since particle emissions from biomass burning are at their highest and aerosol wet removal is at its lowest during the dry season.

The most plausible explanation for the above findings is the existence of a significant ultrafine (< 100 nm diameter) CCN source during the wet season. One such source, not considered by Ross et al. (2003), is the atmospheric new-particle formation (Laakso et al., 2008; Vakkari et al., 2011), which has been observed globally in different environments (e.g. Kulmala et al., 2004). Earlier observations have demonstrated that aerosol particles formed in the atmosphere may produce new CCN in both clean and heavily polluted environments (e.g. Lihavainen et al., 2003; Laaksonen et al., 2005; Kuang et al., 2009; Wiedensohler et al., 2009). The potential importance of atmospheric new particle formation for regional and global CCN budgets has been demonstrated also using global models (Spracklen et al., 2008; Makkonen et al., 2009, 2012; Merikanto et al., 2009; Pierce and Adams, 2007, 2009; Wang and Penner, 2009; Yu and Luo, 2009; Kazil et al., 2010; Luo and Yu, 2011), even though uncertainties related to these studies are still large (Kerminen et al., 2012).

In this study, we investigate CCN production associated with new particle formation over southern Africa, with aim to deepen the understanding on previous observations of Ross et al. (2003). Our main hypothesis is that CCN have different dominant sources during different seasons: atmospheric new particle formation with condensational growth mainly by biogenic vapours during the wet season, and biomass burning or other primary sources during the dry season.

We base our analysis on detailed aerosol measurements, supplemented by trace gas and meteorological observations, conducted over an 18 month period in 2006–2008 at a background surface site in a savannah biome. The analysed CCN production is compared to model simulations with a global aerosol microphysics model GLOMAP (Spracklen et al., 2005).

2 Methods

2.1 Measurements

Measurements were made in the Botsalano game reserve in North-West Province, South Africa ($25°32'28''$ S, $25°45'16''$ E, 1424 a.s.l.). The reserve is located about 50 km north of the nearest city, Mafikeng, with approximately 260 000 inhabitants. One of the largest regional pollution sources in North-West Province, Rustenburg mining region, is located approximately 150 km east of Botsalano. Vegetation of the measurement location is typical for mixed bushveld (Laakso et al., 2008).

The comprehensive measurement description is given by Laakso et al. (2008) and Vakkari et al. (2011) and here we list only briefly the measurements used in this study.

The sub-micron aerosol number size distribution was measured with a Differential Mobility Particle Sizer (Hoppel, 1978; Aalto et al., 2001) in the size range from 10 to 840 nm. The sample was drawn through a Digitel $PM_{2.5}$ inlet (Digitel Elektronik AG, Switzerland). Prior to sizing, the particles were dried with a Nafion-drier (Perma Pure LLC, USA) and then brought to a known charging state with a Ni-63 beta-active neutralizer. The particles were classified with a Vienna-type (length 0.28 m) Differential Mobility Analyzer (Winklmayr et al., 1991) and counted with a TSI Condensation Particle Counter (CPC) model 3010. The time resolution of the system is 7.5 min.

Gases (SO_2, NO_x, CO and O_3) were monitored with one-minute time resolutions using a set of gas analyzers sharing a PTFE-sampling line. Sulphur dioxide was measured with a Thermo-Electron 43S, NO_x with a Teledyne 200AU, CO using a Horiba APMA-360 and ozone with an Environnement s.a. 41A gas analyzer. The gas data were corrected based on on-site multipoint calibrations.

Local meteorological parameters (temperature, potential temperature gradient, relative humidity, wind speed and direction, photosynthetically available radiation (PAR) and amount of precipitation) were logged with a one-minute time resolution. All the instruments were checked and maintained weekly, and a full service was made approximately every three months.

The measurement period utilized in this study started on 23 July 2006 and lasted until 4 February 2008.

2.2 Data analysis methods used on measurement data

The data analyses were carried out using MATLAB program, which was developed to correct the data with calibrations and automatically filter out questionable data. Such values were recorded quite often after frequent electricity breaks.
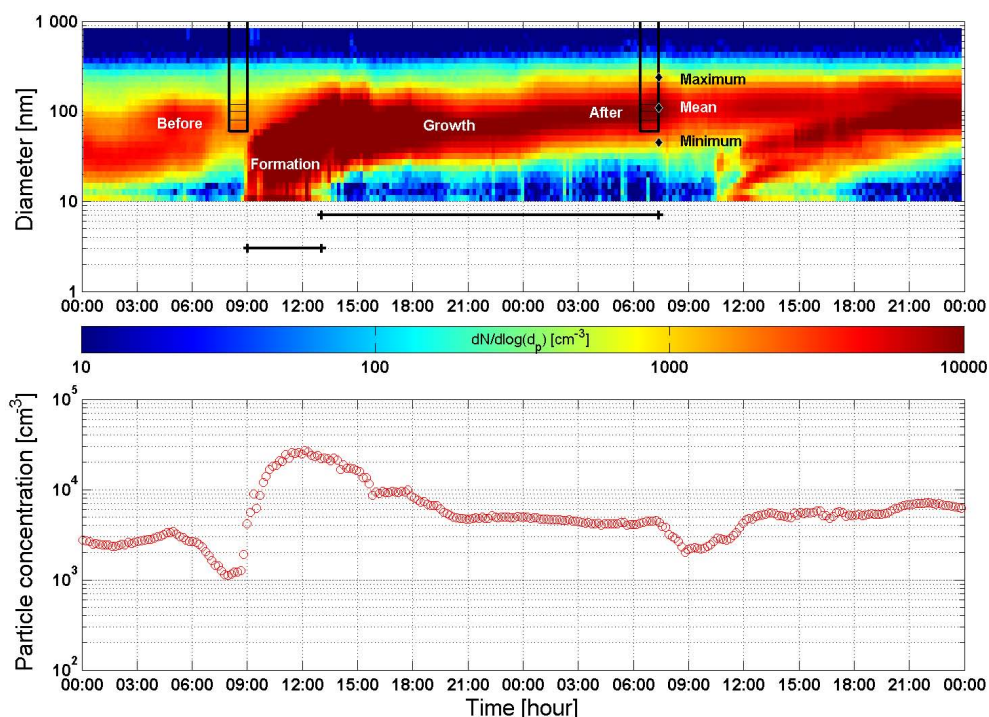
Fig. 1. Evolution of the particle size distribution during a particle formation event showing the different periods where values for analysis are calculated. "Before" is the one hour period before the new 10-nm particles appear, typically just after atmospheric mixing which results in the observed decrease in total particle concentration and breakup of the temperature inversion. "After" is the one hour period at the end of particle growth, but before the start of the next nucleation event. Small horizontal lines in "before" and "after" represent the lower size limits for CCN; 60 nm, 80 nm, 100 nm and 120 nm. "Formation" is the period when 10-nm particles appear whereas "growth" is the period from end of "formation" until "after". The values used are median values for each period. The formation period is not the same as nucleation period as the particles nucleate at sizes of ∼ 1–2 nm. This means the particles appear at 10 nm only approximately 0.5–4 h after they are nucleated.

Furthermore, all the gathered data were checked visually to make sure that the questionable data points were excluded.

The formation rate of 10 nm particles (J_{10}) and particle growth rates (GR) for the size interval 10–30 nm were calculated based on the method described in detail in Dal Maso et al. (2005). This method was also applied to simulated particle size distributions to make the values shown in Fig. 6a and b, and c and d comparable. Values of the condensation sink (CS; Fuchs, 1963), representing the inverse lifetime of non-volatile condensable vapours, were calculated from measured particle number size distributions as in Dal Maso et al. (2005). As the relative humidity at our site is very low during the particle formation and growth period (on average, 37 %), and the hygroscopic growth factors of the particles not known, CS was calculated for dry particle sizes. The hygroscopic growth of ambient aerosol particles is usually quite moderate at relative humidities below 50 % (Zhou, 2001; Laakso et al., 2004; Birmili et al, 2009; Wiedensohler et al., 2012) so our assumption of a dry particle radius should not cause a major error in calculating the value of CS.

To estimate the contribution of sulphuric acid on particle growth we calculated the so-called "sulphuric acid proxy",

[H$_2$SO$_4$]$_{pro}$, based on [SO$_2$], solar radiation intensity and CS (Petäjä et al., 2009, proxy method 1; Vakkari et al., 2011). Since ambient OH radical concentrations are expected to be proportional to the radiation intensity (Rohrer and Berresheim, 2006), [H$_2$SO$_4$]$_{pro}$ is expected to vary as the real gaseous sulphuric acid concentration. However, as this proxy is developed for boreal forest, we consider the absolute values only indicative.

Without direct CCN measurements, we estimated CCN concentrations from particle number size distributions obtained from DMPS measurements by assuming that all particles larger than a certain threshold size act as CCN. Four dry particle threshold sizes (60, 80, 100 and 120 nm) were selected in order to cover different water vapour saturation ratios achieved inside clouds and to take into account the effect of aerosol chemical composition on the CCN activity (Dusek et al., 2006; Hudson, 2007; Quinn et al., 2008). Furthermore, the range of 60–120 nm represents reasonably well the minimum dry diameters of particles observed to act as cloud droplets (Henning et al., 2002; Komppula et al., 2005; Mertes et al., 2005).

Cloud condensation nuclei resulting from new particle formation were determined using the procedure depicted in Fig. 1. After identifying the days with particle formation, we identified the periods with particle formation and growth by visual inspection. In order to characterize the aerosol formation event, we calculated variables such as the number concentrations of particles larger than a certain size before and after the aerosol formation event, the minimum, mean and maximum sizes that the growing particles reach during the event, trace gas concentrations, sulphuric acid proxy and average meteorology during the formation and growth period.

In total, based on our combined measurements (Laakso et al., 2008) we calculated 56 different variables (like average gas concentrations and meteorology) for the formation and growth periods. During most of the days, determination of the end of nucleation mode growth was clear and took place at latest before the atmospheric mixing of next morning started. Due to the selection criteria requiring clear nucleation mode growth, and exclusion of visible air mass property changes, the events utilized in this study are likely to be regional rather than related to individual locations with high emissions. The air mass history was determined using back-trajectories. The hourly 96-h back-trajectories were calculated with the HYSPLIT 4.8 model (Draxler and Hess, 1998, 2004).

2.3 Modelling

We compared the observed data to predictions of the global aerosol model GLOMAP (Spracklen et al., 2005, 2006) which is an extension of the TOMCAT 3-D global chemical transport model (Chipperfield, 2006). GLOMAP is an offline model where the large-scale transport and meteorology is specified from 6-h European Centre for Medium-Range Weather Forecasts (ECMWF) analyses. We ran the model for the same period as the observations (23 July 2006–4 February 2008), with an initial 4 month spin-up. Model microphysical processes include nucleation, coagulation, condensation of gas-phase species, in-cloud and below-cloud aerosol scavenging and deposition, dry deposition and cloud processing (Spracklen et al., 2005).

The model considers two aerosol size distributions described with 20 size bins spanning from 3 nm to 10 μm in dry diameter. One of the distributions is hydrophobic containing freshly emitted organic carbon (OC) and elemental carbon (EC). The other distribution is hydrophilic and contains sulphate, sea salt, and aged OC and EC. The size-resolved CCN concentrations are obtained as the sum of particles exceeding the threshold sizes in the two distributions. The model was run here with a horizontal resolution of $\sim 2.8° \times \sim 2.8°$ and 31 vertical levels between the surface and 10 hPa. The model results were linearly interpolated to the location of the Botsalano measurement station.

Carbonaceous aerosol emissions from large scale biomass burning are obtained from the Global Fire Emission Database version 3 (GFEDv3) (van der Werf et al., 2006) for the same period as the observations. Emission heights were calculated as in Schultz et al. (2008) utilizing the vegetation classification of IGBP. According to the observations (Ito et al., 2007) and GFED database, the burning emissions are strongly seasonal and peak during the dry winter period (June–September) in Southern hemisphere Africa and negligible during the wet season (November–April). Anthropogenic carbonaceous and sulphuric emissions are based on the AEROCOM emission inventories for the year 2000 (Dentener et al., 2006). These emissions are kept constant throughout the year. The applied AEROCOM emissions and assumed particle sizes are explained in more detail in Spracklen et al. (2006). We assumed that 2.5 % of sulphur is emitted as primary sulphate and the remaining sulphur is emitted as SO_2.

Condensable species included in our simulations were sulphuric acid and condensable secondary organics vapours. We assumed that the condensable secondary organic vapours originated entirely from biogenic monoterpenes. Modelled monoterpenes emissions were taken from the GEIA database (Benkovitz et al., 1996) which has a monthly resolution for the emissions. Monoterpenes were oxidized by OH, O_3 and NO_3 to form a first-stage oxidation product (with standard 15 % or doubled 30 % yield, depending on the simulation) that was assumed to condense with a zero vapour pressure onto existing aerosol particles. The secondary organics scheme has been explained in Spracklen et al. (2006).

New particle formation was modelled using separate nucleation schemes for the free troposphere and boundary layer. For the free troposphere we used a binary homogeneous H_2SO_4-H_2O nucleation scheme by Vehkamäki et al. (2002). The model predicts binary homogeneous H_2SO_4-H_2O nucleation to take place mostly in the upper troposphere. For the boundary layer we used either the empirical kinetic H_2SO_4 nucleation scheme (Kuang et al., 2008) with standard secondary organics yield or, alternatively, the scheme involving nucleation of both H_2SO_4 and secondary organics (Paasonen et al., 2010) together with doubled secondary organics production. In the model, the boundary layer nucleation schemes produces in-situ nucleation events at the measurement site, whereas the binary homogeneous H_2SO_4-H_2O nucleation scheme contributes to background particle concentrations through downward transport of free-troposphere particles. In the kinetic H_2SO_4 boundary layer nucleation scheme, the formation rate of 1-nm particles is given by

$$J_1 = k \times [H_2SO_4]^2, \tag{1}$$

where k is the kinetic prefactor. Here we use $k = 2 \times 10^{-12}$ cm^{-6} s^{-1}, that in GLOMAP gives a best agreement, on average, with modelled and observed particle number concentrations in various locations around the world (Spracklen et al., 2010). In the nucleation scheme with H_2SO_4 and secondary organics the formation rate of 2-nm
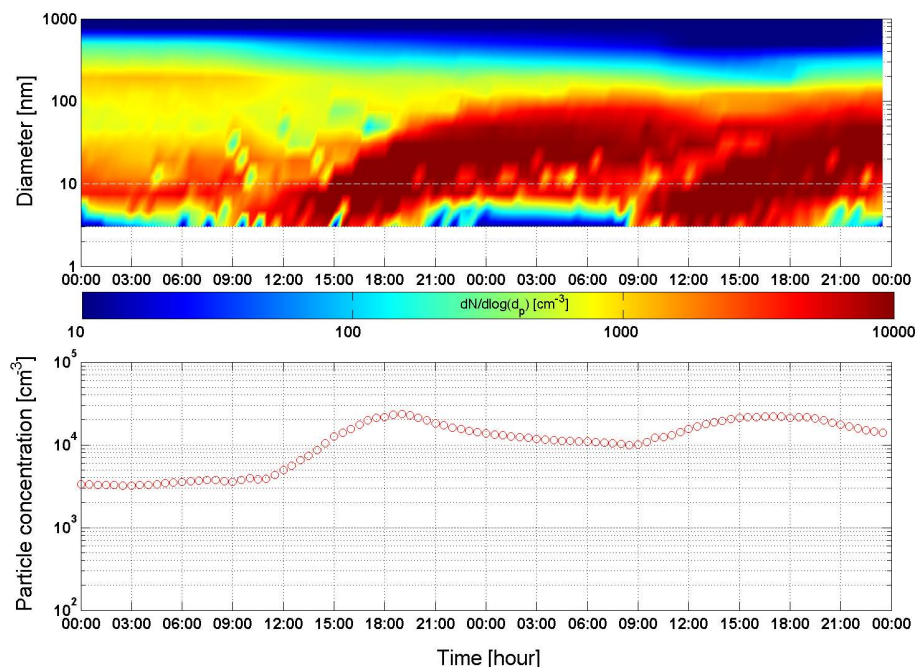
Fig. 2. Modeled evolution of the size distribution during the particle formation event using the particle formation scheme including both sulphuric acid and organics (Eq. 2), and a 30 % secondary organics yield. Total particle number concentration at the lower panel is for the size range 10–1000 nm.

particles is given by

$$J_2 = k_1 \times [H_2SO_4]^2 + k_2 \times [H_2SO_4][\text{nucorg}] + k_3[\text{nucorg}]^2 \quad (2)$$

where [nucorg] is the concentration of organic vapours participating to nucleation. In the model [nucorg] corresponds to the sum of concentrations of all oxidation products of monoterpenes. We use $k_1 = 1.4 \times 10^{-14}\,\text{cm}^{-6}\,\text{s}^{-1}$, $k_2 = 2.6 \times 10^{-14}\,\text{cm}^{-6}\,\text{s}^{-1}$, and $k_3 = 3.7 \times 10^{-16}\,\text{cm}^{-6}\,\text{s}^{-1}$, as recommended by Paasonen et al. (2010).

Both of the nucleation schemes produce particle formation events with roughly the same frequency as the observations. A typical modelled particle formation event (Fig. 2) starts around the mid-day followed by particle growth until the next day, in the same manner as a typical observed particle formation event.

Model simulations were carried out with primary particle emissions only (PR), PR and binary homogeneous nucleation (taking place mainly in upper troposphere) (PR+UTN), and finally also including boundary layer nucleation (PR+UTN+BLN). The impact of different sources was estimated by comparing CCN concentrations between different simulations. In addition, the simulated size distributions were analysed with the visual method described in Sect. 2.2 to allow direct comparisons with observations.

In addition to the runs described above, a sensitivity study varying 28 modelling parameters is included. The details of this study are further discussed in Appendix A and references therein.

3 Results and discussion

3.1 General conditions during measurements

The meteorological characteristics for the site were discussed in detail in Laakso et al. (2008) so we only shortly summarize the results here. Typically, the summer temperatures vary between 15 °C and 30 °C and the winter temperatures between 5 °C and 20 °C. The wet summer season with significantly enhanced biological activity and high VOC emissions (Günther et al., 1995; Otter et al., 2003) is from October until April with some occasional rains outside this period. The dry winter season is characterized by frequent wild fires (Ito et al., 2007) and increased domestic heating by small scale combustion and is typically from late April until early September. September is a spring month which typically represents special characteristics as it is still part of the dry season with high primary emissions, but also with significant biogenic emissions from the vegetation.

In general, most of the precipitation in this area comes in form of intensive rain showers related to thunder storms. During the re-analysis of the Botsalano data, we found that in few cases the precipitation sensor was showing unrealistic high values (Odedina, 2009) with rain intensities above 60 mm h^{-1}. Fortunately, such data are infrequent and the results of our previous article (Laakso et al., 2008) are not significantly changed.
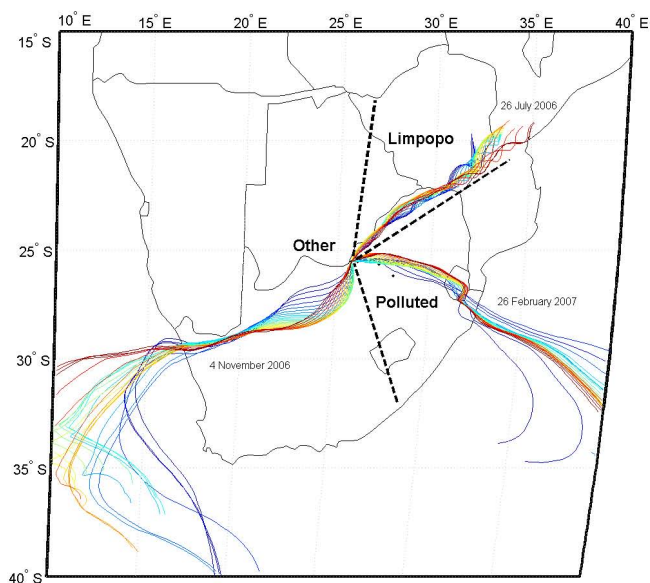
Fig. 3. Hourly 96-h HYSPLIT back trajectories arriving at the measurement site for three example days (24 trajectories for each day) demonstrating the area division used in our analysis. The colours of the trajectories (dark blue → light blue → yellow → red) indicate the hour when each trajectory arrives at Botsalano.

Fig. 4. Monthly median observed (black) and simulated (blue) particle size distributions.

The seasonal meteorology and transport pattern of the region is best illustrated in Garstang et al. (1996). The dominant meteorological conditions are anticyclonic recirculation which dominates during the winter, easterly disturbances frequent in summer and westerly disturbances observed throughout the year. Especially during the anticyclonic recirculation, pollution re-circulates in the atmosphere for up to 20 day long periods.

To check the spatial representativeness of our data, we calculated hourly air mass trajectories for the whole measurement period. Based on visual inspection, we decided to divide the trajectories into three groups based on their origin, typical flow patterns described above, and information from SAFARI 2000 emission inventory. The area division, shown in Fig. 3, is the following: (1) "Polluted": air mass cross over the Rustenburg and/or Johannesburg and/or Vereeniging, (2) "Limpopo": air mass arrives via a trajectory following the northern border of South Africa, but do not cross the industrialized Highveld, and (3) "Other": the trajectories arrive from less populated areas in Karoo and Botswana directions. The reason for this kind of source area classification was the location of the measurement station near the western brink of the polluted Rustenburg-Pretoria-Johannesburg-Vereeniging region. In our location air masses coming from this direction were always polluted, with high SO_2 and accumulation mode particle concentrations. The Botswana-Karoo direction, by contrast, is little influenced by anthropogenic pollution, especially industrial sources. The Limpopo direction is the most common arrival direction and it contains
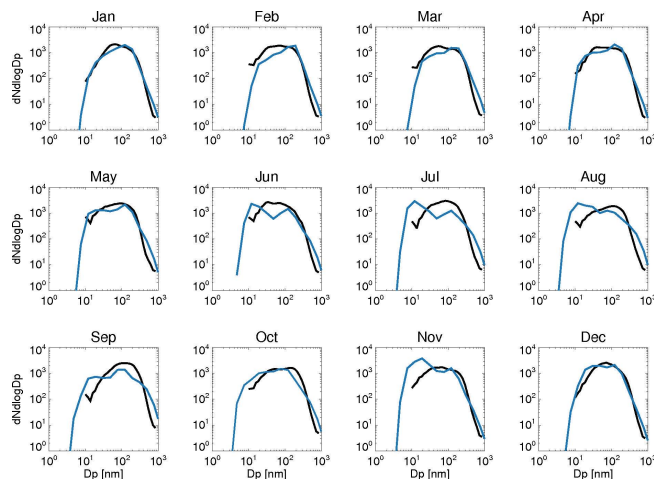
some emissions from domestic biomass burning sources but little industrial pollution.

Based on this analysis, we found no clear annual pattern for the origin of air masses for the days used in our CCN-analysis, which indicates that the potential variation is related to the season rather than differences in flow patterns.

3.2 Aerosol formation and growth rates

During the observation period, clear new particle formation was observed on a total of 254 (or 69 %) of the days (Vakkari et al., 2011). For this study, we chose 187 new particle formation days with a nucleation mode growth up to sizes above 20 nm diameter.

The particle data coverage for the each month varied between 20 % and 100 %, typical monthly data coverage being approximately 80 %. In the whole 18-months data set the data coverage was at least 23 calendar days for each calendar month, which allowed us compare different months and seasons. Assuming similar new particle formation frequency for the days with missing data, days with nucleation with clear growth was found to take place in approximately 50 % of the time.

Figure 4 shows the observed and simulated median particle number size distributions of each calendar month. In general the agreement in the large particle sizes was good, whereas clear differences were seen in smaller sizes that are more sensitive to the aerosol dynamics. This was most visible during the dry period when underestimated particle growth keeps the nucleation mode in small sizes. The monthly-median total particle number concentration (CN) (10–840 nm) and condensation sink (CS) are shown in Fig. 5 while the time series showing the corresponding variabilities are presented in the Appendix (Fig. A2). No clear pattern in differences can be seen: in general the agreement between the observations and simulations was reasonable.
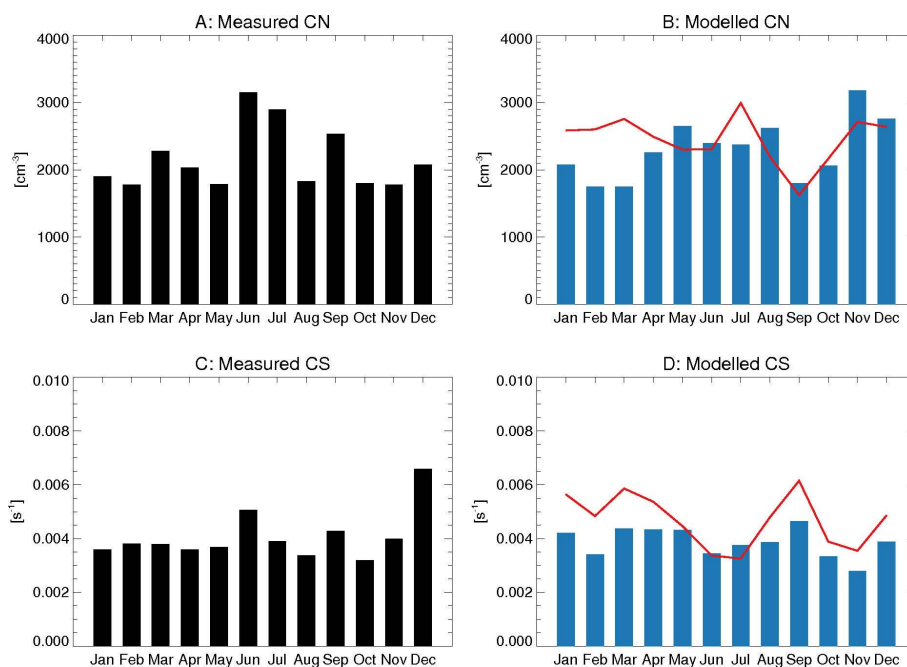
Fig. 5. (A) Monthly median concentration of measured 10–840 nm particles; **(B)** Monthly median concentration of simulated 10–840 nm particles; **(C)** Monthly median observed condensation sink; and **(D)** Monthly median simulated condensation sink. In this and in subsequent figures the bars in the right hand panels indicate the model results with kinetic sulphuric acid nucleation (Eq. 1) and the standard secondary organics scheme, and red lines correspond to results assuming both sulphuric acid and secondary organics nucleation (Eq. 2) and doubled secondary organics scheme.

While the model captured the overall magnitude of the condensation sink quite well, its modeled variability (and hence also the variability in the coagulation sink of the smallest particles) was much lower than the observed one (please see Appendix A).

Figure 6a shows observed 10-nm particle formation rates (Vakkari et al., 2011).

They have a clear minimum during the dry winter season and higher values during the spring and autumn, showing slightly reduced rates during the wet mid-summer. This behaviour is similar to that observed in many other environments (Kulmala et al., 2001; Kerminen et al., 2004; Pierce and Adams, 2007; Kuang et al., 2009; Vakkari et al., 2011), and it can be related to the availability of the condensable vapours participating in the particle formation at ∼ 1 nm size and subsequent growth to 10 nm (the lower limit of DMPS measurement at our site).

Overall, the observed particle formation rates were higher than those typically observed in other remote environments and comparable to or lower than those observed in polluted environments (Kulmala et al., 2004; Kulmala and Kerminen, 2008).

The bars in Fig. 6b represent the modelled 10-nm particle formation rates using the kinetic nucleation scheme (Eq. 1) for 1-nm particles, and subsequent growth to 10 nm sizes. The modelled rates are approximately only 10 % of the observed ones. The kinetic prefactors used in Eqs. (1) and (2)

are known to be uncertain and vary from location to location, but we suspect the main cause for the underestimation of modelled 10-nm particle formation rates to result from the underestimation of nucleating and/or condensing vapours available for these processes, as discussed further below.

Figure 6c shows the observed growth rates of 10–30 nm particles. Similarly to the formation rate, the growth rate has a clear maximum in spring and autumn, a minimum during the dry winter season and a smaller minimum during the wet mid-summer. This cycle is similar to those observed in various other environments (Dal Maso et al., 2005; Qian et al., 2007; Manninen et al., 2010; Pryor et al., 2010; Cheung et al., 2011; Yli-Juuti et al., 2011) and opposite to the annual cycle of estimated sulphuric acid concentrations in Botsalano (Vakkari et al., 2011).

The bars in Fig. 6d represent the modelled particle growth rates. Again, these values are approximately 10–20 % of the observed ones indicating significant underestimation of condensable vapours and overestimation of the pre-existing particle surface. The annual cycle, except for a small midsummer dip, is similar to the observed ones. The smaller growth rate also leads to a larger fraction of depleted particles during the particle growth to 10 nm (Kerminen et al., 2004; Pierce and Adams, 2007; Kuang et al., 2009).

When the simulations data were studied in more detail, we found that unlike in observations, the pre-existing particle concentrations did not show a decrease in accumulation
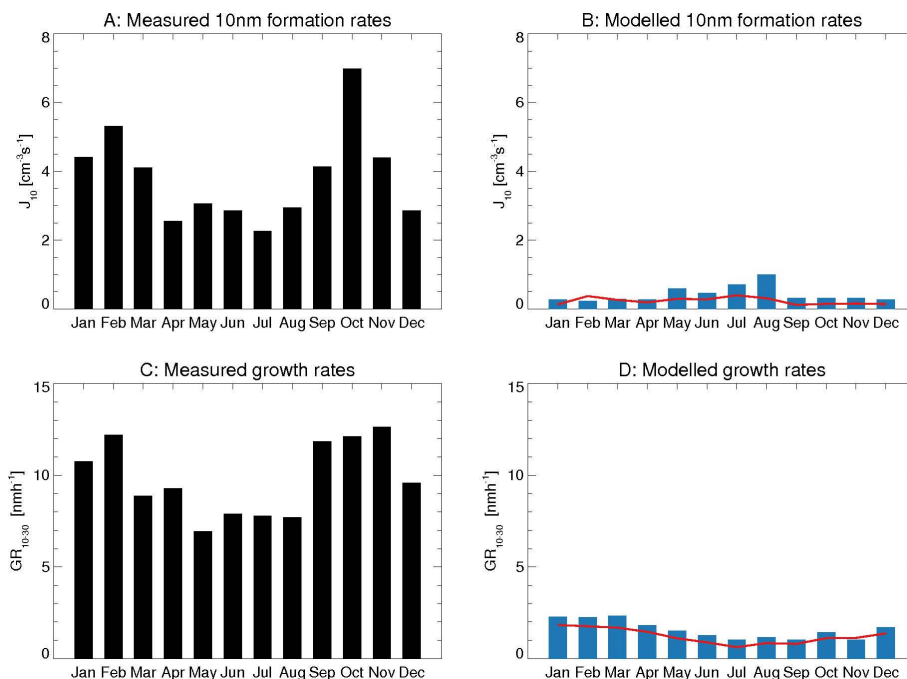
Fig. 6. Observed (left) and modelled (right) particle formation and growth rates. Red curves as in Fig. 5.

mode concentrations during the onset of new particle formation. This is most probably due to the underestimated aerosol removal mechanisms in the residual layer/free troposphere especially during wet season, leading to an overestimation of the condensation to the pre-existing particles and to an underestimation of the CCN production due to boundary layer nucleation. Characteristic for the area, a major fraction of the precipitation comes from multi-cell thunderstorms with strong updrafts (Tyson and Preston-Whyte, 2000), leading to challenges in estimating the particle wet removal mechanism in global models.

The annual cycle of particle growth given by the model follows the observed data and indicates the role biogenic volatile organics have on particle growth. In contrast, the seasonal cycle of modelled J_{10} is different from the one observed ones.

Due to the low growth rates and the wrong seasonal cycle in the particle formation rate, we tested another nucleation scheme including H_2SO_4 and secondary organics (Eq. 2) with the doubled yield of condensable organic vapours (red curves in Fig. 6b and d). The dry season peak in the 10 nm particle formation rate obtained with kinetic H_2SO_4 nucleation was no longer pronounced when the involvement of secondary organics in the nucleation process was included, but the observed peak in the particle formation during the wet season was not produced either (Fig. 6b, red curve). A plausible reason for this would be too slow particle growth. As described in Kerminen et al. (2004), particle survival from 3 to 10 nm is a non-linear competition between growth and scavenging. If particles grow in size too slowly, also the forma-

tion rate of 10 nm particles, despite original nucleation mechanism, is reduced. Doubling the secondary organics yield resulted in an overall shift of both pre-existing and BL nucleated particles to larger sizes, without improving the overall characteristics of particle growth when compared to observations.

The growth rates obtained with the visual method remained nearly equal, or were even slightly reduced (Fig. 6d, red curve). Therefore, it seems that deficiencies in condensable organic emissions alone are not sufficient to explain the differences between the model results and observations.

To further study the deficiencies in the model results, a sensitivity study varying 28 modelling parameters, such as nucleation rates, biomass burning emissions, SOA production, and emitted particle sizes etc., was included using a modal GLOMAP model and Monte Carlo – type emulator of the parameter space (see Appendix for details). The results show that uncertainties in modelled CCN are up to 300 % due to combined uncertainties in the model parameters. The largest sources of uncertainty in the model CCN are due to uncertainties in biomass burning emissions during the dry season, and anthropogenic sulphur emissions during the wet season, due to uncertainties in both in emitted mass and particle sizes.

Biomass burning and anthropogenic sulphur emissions affect modelled nucleation and growth rates that are sensitive to pre-existing particle surface area. Separate sensitivity studies using sectional GLOMAP model with doubled sizes of primary emitted anthropogenic particles roughly doubled model nucleation and growth rates while keeping the total
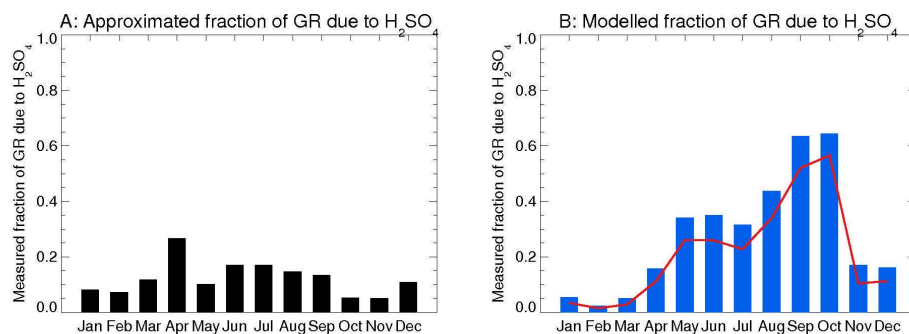
Fig. 7. Approximated fraction of particle growth due to sulphuric acid for observed (left) and simulated (right) results. Red curves as in Fig. 5.

CCN concentrations nearly equal, leading thus to improved results.

Figure 7a shows the seasonal variation of contribution of estimated sulphuric acid on observed particle growth rates (Vakkari et al., 2011). Instead of the absolute value of the proxy, which is less accurate, the main visible feature in the figure is the seasonal cycle: during the wet season the proxy is able to explain a smaller fraction of the particle growth than during the dry season, indicating the contribution of some non-sulphuric acid vapours in the particle growth. The same pattern is also visible in modelled data (Fig. 7b, bars and red curve), supporting the role of other vapours like organic compounds (Kanikidou et al., 2005; Metzger et al., 2010; Riipinen et al., 2011; Yu, 2011) in the seasonal cycle of the particle growth.

3.3 CCN-sized particle formation via new particle formation

Figure 8 shows the monthly measured and simulated concentration of CCN-sized particles and the relative increases of particle concentrations due to new particle formation and growth. Both observations and model results show a similar absolute number of different CCN-sized particles, particularly from October to March. The main difference is the dry winter period, when the model indicates lower concentrations than observed. A possible explanation for this difference is the underestimated wild fire emissions, for which the model uncertainties are large (see Appendix).

The increase in CCN-sized particle concentration was further analysed by applying the method described in Fig. 1 to both observed and modelled particle data.

Figure 8c and d show the enhancement factor of CCN-sized particles due to new particle formation. The factor was obtained by dividing the number of CCN-sized particles after a particle formation event by that prior to the event. Both observations and model show that new particle formation was not able to affect the CCN-concentrations during the dry seasons, regardless of the model nucleation scheme. In contrast, the observations show a significant increase of these particles

during the wet season. This suggests that new particle formation is a significant source of CCN-sized particles during the wet season. In model results, this increase is not seen due to lack of particle growth.

In the observation data, the CCN production by nucleation during the wet seasons is likely a result of multiple factors. Besides the higher growth rates, one of them was the fact that the value of CS (resulting mainly from CCN-sized particles) during the morning inversion breakup just before the new particle formation event was almost two times higher during the dry season (4.5×10^{-3} s^{-1}) than during the wet season (2.6×10^{-3} s^{-1}). The reason for the greater CS during the dry season is likely due to anticyclonic re-circulation limiting the venting of pollution, limited in-cloud and below-cloud scavenging and greater biomass burning emissions.

The modelling results were also analysed by simulating particle concentrations without boundary layer new particle formation, and without any particle formation at all. The resulting CCN-sized particle concentrations without BL nucleation were clearly lower during the wet season (Fig. 8b).

Also, the model runs containing only primary emission (when compared with the two other cases) suggests that particles originating from upper tropospheric nucleation have a significant contribution on simulated CCN concentrations throughout the year. This suggests that the enhancement factor obtained from the visual analysis of the measurement data is likely to underestimate the total effect of new particle formation on CCN concentrations. There are two reasons for this: first, in the visual analysis the effects of particle formation over longer time periods than the duration of a single particle formation event are not accounted for; second, the flux of nucleated particles originating from upper troposphere cannot be quantified by the visual analysis method used in this paper.

Figure 9 shows the minimum, mean and maximum size of particles in the nucleation mode at the end of growth in observations (Fig. 9a) and simulations (Fig. 9b) obtained as explained in Fig. 1. Clearly, the particles reached larger sizes during the wet season (see also Fig. 6a, b). Since the value of CS during the period of particle growth did not
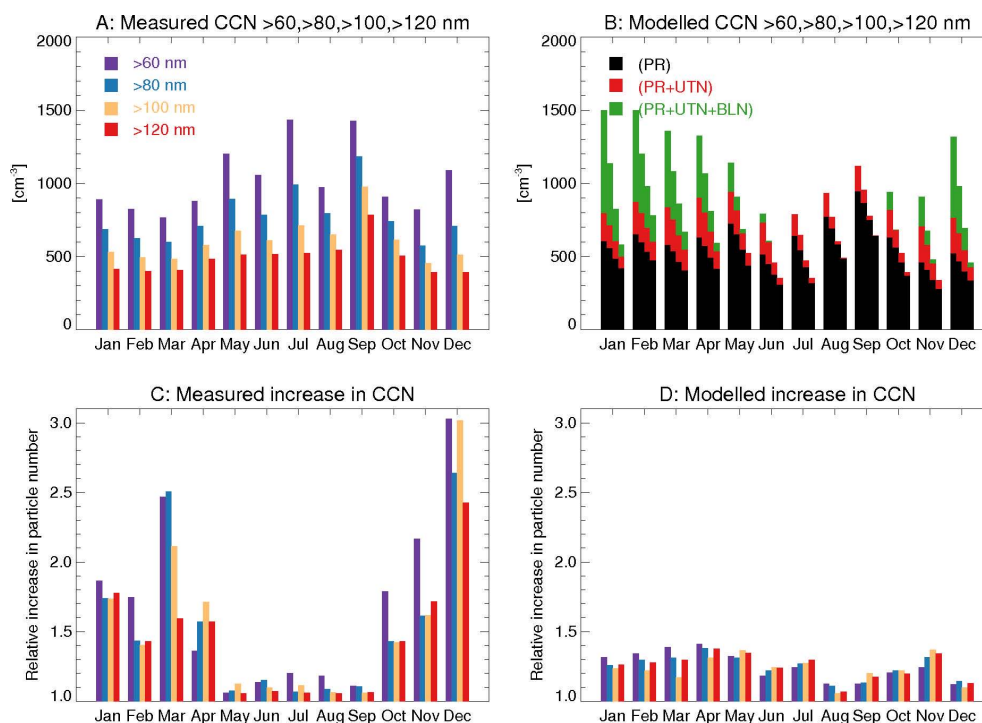
Fig. 8. (A) Measured monthly median concentration of particles above 60 nm, 80 nm, 100 nm and 120 nm; **(B)** Modelled monthly median concentration of particles above 60 nm, 80 nm, 100 nm and 120 nm using kinetic sulphuric acid nucleation (Eq. 1) and the standard secondary organics scheme; **(C)** Observed relative increase of CCN-sized particles (median); and **(D)** Simulated relative increase of CCN-sized particles with kinetic sulphuric acid nucleation and the standard secondary organics (median).
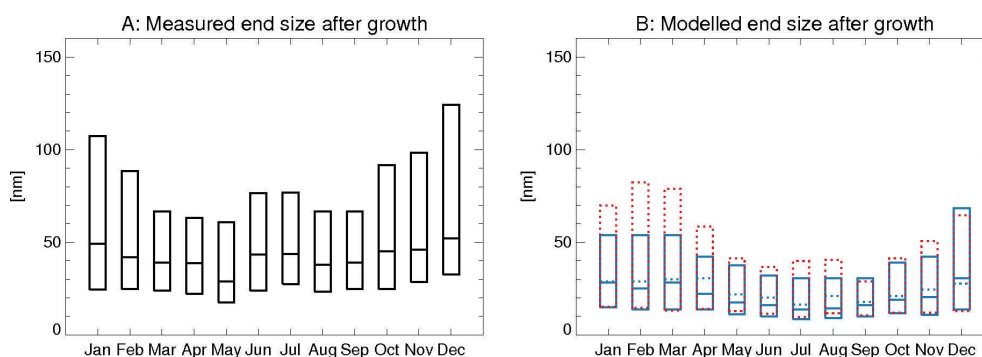

Fig. 9. Smallest, mean and max size of growing nucleation mode at the end of the event **(A)** in observations; and **(B)** simulations with kinetic sulphuric acid nucleation (Eq. 1) and the standard secondary organics scheme. Dashed bars on the right represent end-sizes assuming both sulphuric acid and secondary organics nucleation (Eq. 2) and doubled secondary organics scheme.

vary significantly between the different seasons (Fig. 4c and Vakkari et al., 2011), the larger end size of nucleated particles during the wet season is mainly due to higher condensable vapour concentrations at that time of the year. This comparison clearly reveals the difference in particle growth: in the simulations the particles are not able to grow effectively enough above our lowest threshold size (60 nm) and to make a significant contribution to CCN concentrations. Another difference between the observed and simulated new particle formation was the longer time it took for particles to

appear at 10 nm in the simulations (on average 7.5 h in simulations against observed 4 h). This feature was related to the under-estimated particle growth at sizes below 10 nm.

Another look to the simulation data is presented in Fig. 10 which illustrates the predicted CCN concentration at 0.3 % supersaturation. The seasonal impact of boundary layer nucleation on composition-resolved CCN concentrations is similar to size-resolved CCN concentrations, supporting the size-resolved CCN counting method used in analysis of observations. Also in case of composition-resolved CCN,
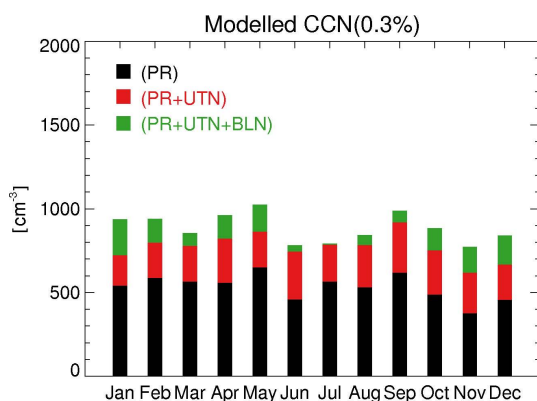
Fig. 10. Modelled size and composition resolved CCN concentrations at 0.3 % supersaturation when accounting for the composition of particles by using a hygroscopicity parameter, κ (Petters and Kreidenweis, 2007), for the kinetic sulphuric acid nucleation (Eq. 1) and the standard secondary organics scheme.

modelled boundary layer nucleation made a significant contribution during the wet season.

4 Conclusions

This study investigated the effect of new particle formation on CCN concentrations in a savannah environment in southern Africa. The observations show clearly that during the wet season, a fraction of CCN-sized particles originates from boundary layer new particle formation, whereas primary particulate sources dominate during the dry winter season. The large contribution of boundary layer nucleation to wet season CCN concentrations is mainly due to high particle formation and growth rates combined with the smaller concentration of pre-existing CCN (due to mixing of cleaner air from above). Based on the estimated seasonal cycle of sulphuric acid and biomass burning emissions, and earlier studies on BVOC emissions in Southern Africa (e.g. Otter et al., 2003), we assume that the higher growth rates during the wet season may be attributed to condensable vapours of biogenic origin.

The comparison of observations and modelling results revealed several interesting results. First of all, earlier analysis (Spracklen et al., 2010) showed that GLOMAP produced realistic concentrations of CCN-sized particles in diverse environments including our measurement site Botsalano. However, when the contribution of one of the mechanisms producing CCN, boundary layer nucleation, was studied, we found that the number of CCN produced via BL nucleation was significantly different from the observations.

This leads us to the following hypothesis: in an environment with enough solar radiation, precursors and seasonal variability, there is a pool of CCN which is filled by competing mechanisms: primary emissions during the dry season and secondary particle formation when pre-existing particle surface is reduced. If in a model the physical mechanisms are correct, but magnitude of either primary emissions or nucleating/condensing vapours are incorrect, we may get a relative correct number concentration of CCN, but for wrong reasons or due to wrong sources.

A sensitivity analysis of the model results shows that combined uncertainties in the model input lead to very high uncertainties in the model CCN, as described in the Appendix A. The uncertainties in CCN result primarily from the uncertainties in biomass burning emissions during the dry season, and anthropogenic sulphur emissions during the wet season. These uncertainties affect the particle formation and growth rates via the pre-existing particle surface area and its variability. Sensitivity runs with doubled organic production and a different nucleation mechanism did not suggest that these could be the main sources of underestimated formation and growth rates of particles.

Additionally, by looking at the duration of new particle formation in simulation and observations, we found that on average, simulations showed approximately twice as long duration (at 10 nm size) than observations (7.5 h against 4 h). This longer than observed duration of nucleation, partly due to underestimated growth rates leads to and increased coagulation loss of particles. These features may be due to the deficiencies in diurnal cycle of organic emissions, or too slow oxidation reactions leading to underestimation of condensable vapours in the morning. Another possibility involves unexplored chemical reactions between biogenic compounds and anthropogenic SO_2 during the wet season. For example, terpenes have been shown to initiate significant non-OH related sulphuric acid production when SO_2 is present (Mauldin III et al., 2012), and the same chemistry might also be able to produced low-volatile organic vapours needed for the growth of freshly-nucleated particles.

Process-level understanding of the CCN formation is essential for reliable predictions of historical and future changes in the indirect aerosol forcing. According to our results the models can predict modern-day CCN concentrations reasonably well, while not capturing the relative importance of different CCN sources. The uncertainties appear to be mostly related to uncertainties in primary particle emissions, including the emissions variability, rather than to the nucleation mechanism or SOA production. Due to multiple sources of uncertainties in the model input parameters, we see a need for long-term organic vapour observations to quantify the concentrations of biogenic and anthropogenic organic vapour over Southern Africa and additionally, continuous observations of boundary layer and free troposphere aerosol particle concentrations. Additionally, we recommend the verification of global models based on fluxes in and out of system rather than concentrations resulting from these fluxes.

Appendix A

Sensitivity analysis of modelled CCN

We investigated the model uncertainties leading to differences between the observations and simulations with a sensitivity analysis of global CCN concentrations based on the approach of Lee et al. (2012, 2013). In these previous studies we quantified the sensitivity to 8 uncertain parameters. Here we extended the analysis to 28 parameters (Lee et al., 2013). The sensivity study was carried out using the modal version of the GLOMAP model (Mann et al., 2010), while the sectional version was used in other parts of this paper. Both models are in good agreement in terms of global CCN (Mann et al., 2012).

The ensemble of 168 one-year model simulations covers the full uncertainty space of the parameters describing e.g. emissions of sea spray, primary BCOC from wildfires, biomass burning, fossil fuel and biofuel combustion, boundary layer and free tropospheric nucleation rates, biogenic and anthropogenic SOA production, anthropogenic and natural sulphur sources, aerosol-cloud interaction parameters and structures of the aerosol model, with the choice of parameters and their ranges based on expert elicitation (see Lee et al., 2013 for details). A Gaussian Process emulator conditioned on the model data was used to generate continuous model output across the parameter space for each grid cell of the model. This approach enables a Monte Carlo-type sampling of the model uncertainty space and a variance-based sensitivity analysis of the modelled CCN. The main output in each grid cell of the model is a probability density function of CCN, from which the total variance as well as variance contributions of the uncertain parameters can be computed.

The upper panel in Fig. A1 shows the monthly mean CCN concentration at Botsalano together with the 2-sigma range accounting for the uncertainties in the model parameters. The lower panel represents the contribution of each parameter to the total variance in CCN at this site. From May to December the main source of uncertainty is biomass burning. The absolute number of CCN shown in Fig. A1 is not directly comparable with those shown in the paper because of the different calculation method, but they do provide an indication of the likely sources of uncertainty. First, Fig. A1 assumes a CCN diameter of 50 nm, which is smaller than used in the main paper. Second, Fig. A1 refers to an altitude of 915 hPa. Third, we would not expect the mean model from the ensemble to agree with any single run using this bin model. Despite these differences, the processes leading to the uncertainties are the same.

The sensitivity study shows two parameters dominating the uncertainty in the total CCN concentrations: the biomass burning emission mass flux (parameter BB_EMS) and the size of the emitted particles (BB_DIAM). BB_EMS was assumed to be uncertainty within a factor 0.25/4 and BB_DIAM was assumed to be uncertainty between 50 and
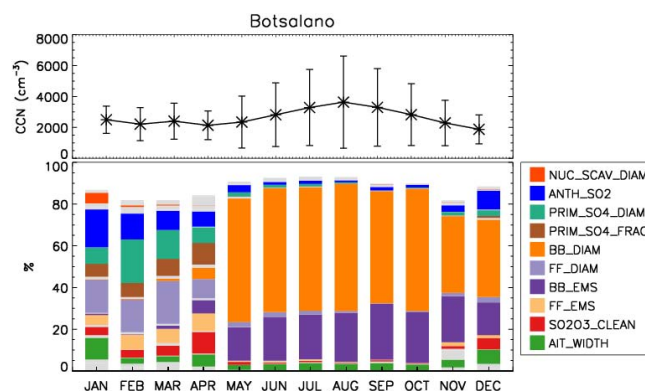

Fig. A1. Upper panel: the seasonal cycle of CCN concentrations at the surface at the Botsalano site together with the 2-sigma uncertainty range due to uncertainty in 28 model parameters. Lower panel: the fraction of variance in CCN attributable to various emissions and processes, indicated by the colour key.

200 nm dry diameters. The 2-sigma CCN uncertainty range in this period is $\pm 3000 \, \text{cm}^{-3}$. Outside the biomass burning season the sources of CCN uncertainty are quite different and the overall uncertainty is lower (of the order $\pm 1000 \, \text{cm}^{-3}$). In this season, the main sources of uncertainty are sub-grid sulphate particles from anthropogenic sources (PRIM_SO4_DIAM and PRIM_SO4_FRAC), the anthropogenic SO$_2$ emissions (ANTH_SO2) and fuel-derived aerosol (FF_DIAM and FF_EMS).

In addition to the model sensitivity analysis, we also looked at the actual time series of observed and simulated total number concentrations (Fig. A2a) and condensation sink (Fig. A2b). These time series show a difficult-to-address phenomena related to the particle formation dynamics: especially for Africa, most emission inventories are less accurate and can provide only limited temporal resolution, leading to use of average emissions based on monthly emissions. However, as visible in Fig. A2b, variability of observed condensation sink (with average CS of $5.4 \times 10^{-3} \, \text{s}^{-1}$ and standard deviation of $4.5 \times 10^{-3} \, \text{s}^{-1}$) is significantly higher than that of simulated variability (with average CS of $4.0 \times 10^{-3} \, \text{s}^{-1}$ and standard deviation of $1.4 \times 10^{-3} \, \text{s}^{-1}$). Now as the survival rate of fresh particles is exponentially proportional to pre-existing particle surface (Kulmala and Kerminen, 2008), the lack of day-to-day variability of the current emission inventories may have a significant, non-linear effect on new particle formation characteristics.
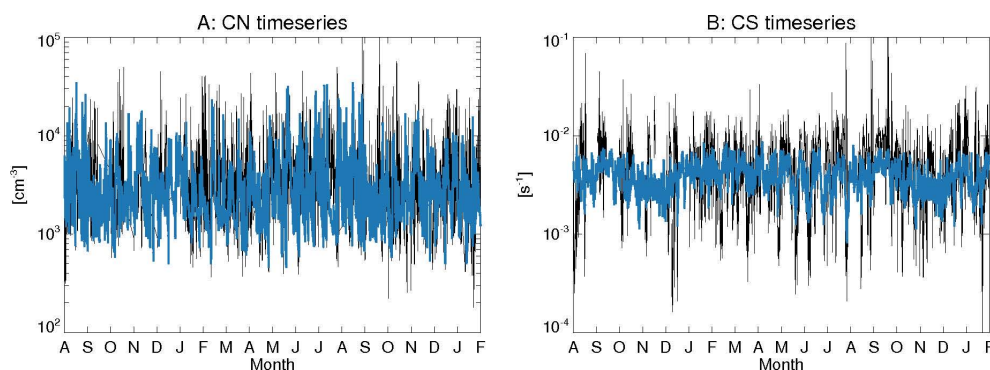
Fig. A2. Simulated (blue) and observed (black) time series of: **(A)** 10–840 nm particles and **(B)** condensation sink for the period from 1 August 2006 to 31 January 2008.

References

Aalto, P., Hämeri, K., Becker, E., Weber, R., Salm, J., Mäkelä, J. M., Hoell, C., O'Dowd, C. D., Karlsson, H., Hansson, H.-C., Väkevä, M., Koponen, I. K., Buzorius, G., and Kulmala, M.: Physical characterization of aerosol particles during nucleation events, Tellus, 53B, 344–358, 2001.

Andreae, M. O. and Rosenfeld, D.: Aerosol-cloud-precipitation interactions. Part 1. The nature and sources of cloud-active aerosols, Earth-Sci. Rev., 89, 13–41, 2008.

Benkovitz, C., Scholtz, M., Pacyna, J., Tarrasón, L., Dignon, J., Voldner, E., Spiro, P., Logan, J., and Graedel, T.: Global gridded inventories of anthropogenic emissions of sulfur and nitrogen, J. Geophys. Res., 101, 29239–29253, 1996.

Birmili, W., Schwirn, K., Nowak, A., Petäjä, T., Joutsensaari, J., Rose, D., Wiedensohler, A., Hämeri, K., Aalto, P., Kulmala, M., and Boy, M.: Measurements of humidified particle number size distributions in a Finnish boreal forest: derivation of hygroscopic particle growth factors, Boreal Environ. Res., 14, 458–480, 2009.

Cheung, H. C., Morawska, L., and Ristovski, Z. D.: Observation of new particle formation in subtropical urban environment, Atmos. Chem. Phys., 11, 3823–3833, doi:10.5194/acp-11-3823-2011, 2011.

Chipperfield, M.: New version of the TOMCAT/SLIMCAT offline chemical transport model: intercomparison of stratospheric tracer experiments, Q. J. Roy. Meteorol. Soc., 132, 1179–1203, doi:10.1256/qj.05.51, 2006.

Dal Maso, M., Kulmala, M., Riipinen, I., Wagner, R., Hussein, T., Aalto, P. P., and Lehtinen, K. E. J.: Formation and growth of fresh atmospheric aerosols: eight years of aerosol size distribution data from SMEAR II, Hyytiälä, Finland, Boreal Environ. Res., 10, 323–336, 2005.

Dentener, F., Kinne, S., Bond, T., Boucher, O., Cofala, J., Generoso, S., Ginoux, P., Gong, S., Hoelzemann, J. J., Ito, A., Marelli, L., Penner, J. E., Putaud, J.-P., Textor, C., Schulz, M., van der Werf, G. R., and Wilson, J.: Emissions of primary aerosol and precursor gases in the years 2000 and 1750 prescribed data-sets for AeroCom, Atmos. Chem. Phys., 6, 4321–4344, doi:10.5194/acp-6-4321-2006, 2006.

Draxler, R. R. and Hess, G. D.: An overview of the HYSPLIT_4 modeling system for trajectories, dispersion and deposition, Aust. Meteorol, Mag., 47, 295–308, 1998.

Draxler, R. R. and Hess, G. D.: Description of the HYSPLIT_4 Modeling System, NOAA Technical Memorandum ERL ARL-224, 2004.

Dusek, U., Frank, G. P., Hildebrandt, L., Curtius, J., Schneider, J., Walter, S., Chand, D., Drewnick, F., Hings, S., Jund, D., Borrmann, S., and Andreae, M. O.: Size matters more than chemistry for cloud-nucleating ability of aerosol particles, Science, 312, 1375–1378, 2006.

Fuchs, N. A.: On the Stationary Charge Distribution on, Aerosol Particles in a Bipolar Ionic Atmosphere, Geophys. Pure Appl., 56, 185–193, 1963.

Garstang, M., Tyson, M., Swap, R., Edwards, M., Kållberg, P., and Lindesay, J. A.: Horizontal and vertical transport of air over southern Africa, J. Geophys. Res., 101, 23721–23736, 1996.

Günther, A., Hewitt, C., Erickson, D., Geron, C., Graedal, T., Harley, P., Klinger, L., Lerdau, M., McKay, W., Pierce, T., Scholes, B., Steinbrecher, R., Tallamraju, R., Taylor, J., and Zimmerman, P.: A global model of natural volatile organic compound emissions, J. Geophys. Res., 100, 8873–8892, 1995.

Henning, S., Weingartner, E., Schmidt, S., Wendisch, M., Gäggeler, H. W., and Baltensperger, U.: Size-dependent aerosol activation at the high-alpine site Jungfraujoch (3580 m asl), Tellus, 54B, 82–95, 2002.

Hoppel, W. A.: Determination of the aerosol size distribution from the mobility distribution of the charged fraction of aerosols, J. Aerosol Sci., 9, 41–54, 1978.

Hudson, J. G.: Variability of the relationship between particle size and cloud-nucleating ability, Geophys. Res. Lett., 34, L08801, doi:10.1029/2006GL028850, 2007.

IPCC: Summary for Policymakers, in: Climate Change 2007: The Physical Science Basis. Contribution of Working Group I to the Fourth Assessment Report of the Intergovernmental Panel on

Climate Change, edited by: Solomon, S., Qin, D., Manning, M., Chen, Z., Marquis, M., Averyt, K. B., Tignor, M., and Miller, H. L., Cambridge University Press, Cambridge, United Kingdom and New York, NY, USA, 2007.

Ito, A., Ito, A., and Akimoto, H.: Seasonal and interannual variations in CO and BC emissions from open biomass burning in Southern Africa during 1998–2005, Global Biogeochem. Cy., 21, GB2011, doi:10.1029/2006GB002848, 2007.

Jones, T. A., Christopher, S. A., and Quaas, J.: A six year satellite-based assessment of the regional variations in aerosol indirect effects, Atmos. Chem. Phys., 9, 4091–4114, doi:10.5194/acp-9-4091-2009, 2009.

Kanakidou, M., Seinfeld, J. H., Pandis, S. N., Barnes, I., Dentener, F. J., Facchini, M. C., Van Dingenen, R., Ervens, B., Nenes, A., Nielsen, C. J., Swietlicki, E., Putaud, J. P., Balkanski, Y., Fuzzi, S., Horth, J., Moortgat, G. K., Winterhalter, R., Myhre, C. E. L., Tsigaridis, K., Vignati, E., Stephanou, E. G., and Wilson, J.: Organic aerosol and global climate modelling: a review, Atmos. Chem. Phys., 5, 1053–1123, doi:10.5194/acp-5-1053-2005, 2005.

Kazil, J., Stier, P., Zhang, K., Quaas, J., Kinne, S., O'Donnell, D., Rast, S., Esch, M., Ferrachat, S., Lohmann, U., and Feichter, J.: Aerosol nucleation and its role for clouds and Earth's radiative forcing in the aerosol-climate model ECHAM5-HAM, Atmos. Chem. Phys., 10, 10733–10752, doi:10.5194/acp-10-10733-2010, 2010.

Kerminen, V.-M., Lehtinen, K. E. J., Anttila, T., and Kulmala, M.: Dynamics of atmospheric nucleation mode particles: a timescale analysis, Tellus, 56B, 135–146, 2004.

Kerminen, V.-M., Paramonov, M., Anttila, T., Riipinen, I., Fountoukis, C., Korhonen, H., Asmi, E., Laakso, L., Lihavainen, H., Swietlicki, E., Svenningsson, B., Asmi, A., Pandis, S. N., Kulmala, M., and Petäjä, T.: Cloud condensation nuclei production associated with atmospheric nucleation: a synthesis based on existing literature and new results, Atmos. Chem. Phys., 12, 12037–12059, doi:10.5194/acp-12-12037-2012, 2012.

Khain, A. P.: Notes on state-of-the-art investigations of aerosol effects on precipitation: a critical review, Environ. Res. Lett., 4, 015004, doi:10.1088/1748-9326/4/1/015004, 2009.

Komppula, M., Lihavainen, H., Kerminen, V.-M., Kulmala, M., and Viisanen, Y.: Measurements of cloud droplet activation of aerosol particles at a clean subarctic background site, J. Geophys. Res., 110, D06204, doi:10.1029/2004JD005200, 2005.

Kuang, C., McMurry, P. H., McCormick, A. V., and Eisele F. L.: Dependence of nucleation rates on sulfuric acid vapor concentration in diverse atmospheric locations, J. Geophys. Res., 113, D10209, doi:10.1029/2007JD009253, 2008.

Kuang, C., McMurry, P. H., and McCormick, A. V.: Determination of cloud condensation production form measured new particle formation events, Geophys. Res. Lett., 36, l09822, doi:10.1029/2009GL037584, 2009.

Kulmala, M. and Kerminen, V.-M.: On the formation and growth of atmospheric nanoparticles, Atmos. Res., 90, 132–150, 2008.

Kulmala, M., Dal Maso, M., Mäkelä, J. M., Pirjola, L., Väkevä, M., Aalto, P., Miikkulainen, P., Hämeri, K., and O'Dowd, C. D.: On the formation, growth and composition of nucleation mode particles, Tellus, 53B, 479–490, 2001.

Kulmala, M., Vehkamaki, H., Petaja, T., Dal Maso, M., Lauri, A., Kerminen, V.-M., Birmili, W., and McMurry, P. H.: Formation

and growth of ultrafine atmospheric particles: a review of observations, J. Aerosol Sci., 35, 143–176, 2004.

Laakso, L., Petäjä, T., Lehtinen, K. E. J., Kulmala, M., Paatero, J., Hõrrak, U., Tammet, H., and Joutsensaari, J.: Ion production rate in a boreal forest based on ion, particle and radiation measurements, Atmos. Chem. Phys., 4, 1933–1943, doi:10.5194/acp-4-1933-2004, 2004.

Laakso, L., Laakso, H., Aalto, P. P., Keronen, P., Petäjä, T., Nieminen, T., Pohja, T., Siivola, E., Kulmala, M., Kgabi, N., Molefe, M., Mabaso, D., Phalatse, D., Pienaar, K., and Kerminen, V.-M.: Basic characteristics of atmospheric particles, trace gases and meteorology in a relatively clean Southern African Savannah environment, Atmos. Chem. Phys., 8, 4823–4839, doi:10.5194/acp-8-4823-2008, 2008.

Laaksonen, A., Hamed, A., Joutsensaari, J., Hiltunen, L., Cavalli, F., Junkermann, W., Asmi, A., Fuzzi, S., and Facchini, M. C.: Cloud condensation nucleus production from nucleation events at a highly polluted region, Geophys. Res. Lett., 32, L06812, doi:10.1029/2004GL022092, 2005.

Lee, L. A., Carslaw, K. S., Pringle, K. J., Mann, G. W., and Spracklen, D. V.: Emulation of a complex global aerosol model to quantify sensitivity to uncertain parameters, Atmos. Chem. Phys., 11, 12253–12273, doi:10.5194/acp-11-12253-2011, 2011.

Lee, L. A., Carslaw, K. S., Pringle, K. J., and Mann, G. W.: Mapping the uncertainty in global CCN using emulation, Atmos. Chem. Phys., 12, 9739–9751, doi:10.5194/acp-12-9739-2012, 2012.

Lee, L. A., Carslaw, K. S., Pringle, K. J., Mann, G. W., Spracklen, D. V., Pierce, J. A. and Carslaw, K. S.: The magnitude and causes of uncertainty in global model predictions of CCN, Atmos. Chem. Phys. Discuss., in press, 2013.

Lihavainen, H., Kerminen, V.-M., Komppula, M., Hatakka, J., Aaltonen, V., Kulmala, M., and Viisanen, Y.: Production of "potential" cloud concensation nuclei associated with atmospheric new-particle formation in northern Finland, J. Geophys. Res., 108, 4782, doi:10.1029/2003JD003887, 2003.

Luo, G. and Yu, F.: Sensitivity of global cloud condensation nuclei concentrations to primary sulfate emission parameterizations, Atmos. Chem. Phys., 11, 1949–1959, doi:10.5194/acp-11-1949-2011, 2011.

Makkonen, R., Asmi, A., Korhonen, H., Kokkola, H., Järvenoja, S., Räisänen, P., Lehtinen, K. E. J., Laaksonen, A., Kerminen, V.-M., Järvinen, H., Lohmann, U., Bennartz, R., Feichter, J., and Kulmala, M.: Sensitivity of aerosol concentrations and cloud properties to nucleation and secondary organic distribution in ECHAM5-HAM global circulation model, Atmos. Chem. Phys., 9, 1747–1766, doi:10.5194/acp-9-1747-2009, 2009.

Makkonen, R., Asmi, A., Kerminen, V.-M., Boy, M., Arneth, A., Guenther, A., and Kulmala, M.: BVOC-aerosol-climate interactions in the global aerosol-climate model ECHAM5.5-HAM2, Atmos. Chem. Phys., 12, 10077–10096, doi:10.5194/acp-12-10077-2012, 2012.

Mann, G. W., Carslaw, K. S., Spracklen, D. V., Ridley, D. A., Manktelow, P. T., Chipperfield, M. P., Pickering, S. J., and Johnson, C. E.: Description and evaluation of GLOMAP-mode: a modal global aerosol microphysics model for the UKCA composition-climate model, Geosci. Model Dev., 3, 519–551, doi:10.5194/gmd-3-519-2010, 2010.

Mann, G. W., Carslaw, K. S., Ridley, D. A., Spracklen, D. V., Pringle, K. J., Merikanto, J., Korhonen, H., Schwarz, J. P., Lee,

L. A., Manktelow, P. T., Woodhouse, M. T., Schmidt, A., Breider, T. J., Emmerson, K. M., Reddington, C. L., Chipperfield, M. P., and Pickering, S. J.: Intercomparison of modal and sectional aerosol microphysics representations within the same 3-D global chemical transport model, Atmos. Chem. Phys., 12, 4449–4476, doi:10.5194/acp-12-4449-2012, 2012.

Manninen, H. E., Nieminen, T., Asmi, E., Gagné, S., Häkkinen, S., Lehtipalo, K., Aalto, P., Vana, M., Mirme, A., Mirme, S., Hõrrak, U., Plass-Dülmer, C., Stange, G., Kiss, G., Hoffer, A., Törő, N., Moerman, M., Henzing, B., de Leeuw, G., Brinkenberg, M., Kouvarakis, G. N., Bougiatioti, A., Mihalopoulos, N., O'Dowd, C., Ceburnis, D., Arneth, A., Svenningsson, B., Swietlicki, E., Tarozzi, L., Decesari, S., Facchini, M. C., Birmili, W., Sonntag, A., Wiedensohler, A., Boulon, J., Sellegri, K., Laj, P., Gysel, M., Bukowiecki, N., Weingartner, E., Wehrle, G., Laaksonen, A., Hamed, A., Joutsensaari, J., Petäjä, T., Kerminen, V.-M., and Kulmala, M.: EUCAARI ion spectrometer measurements at 12 European sites – analysis of new particle formation events, Atmos. Chem. Phys., 10, 7907–7927, doi:10.5194/acp-10-7907-2010, 2010.

Mauldin III, R. L., Berndt, T., Sipilä, M., Paasonen, P., Petäjä, T., Kim, S., Kurtén, T., Stratmann, F., Kerminen, V.-M., and Kulmala, M.: A new atmospherically relevant oxidant of sulphur dioxide, Nature, 488, 193–196, doi:10.1038/nature11278, 2012.

Merikanto, J., Spracklen, D. V., Mann, G. W., Pickering, S. J., and Carslaw, K. S.: Impact of nucleation on global CCN, Atmos. Chem. Phys., 9, 8601–8616, doi:10.5194/acp-9-8601-2009, 2009.

Mertes, S., Lehmann, K., Nowak, A, Massling, A, and Wiedensohler, A.: Link between aerosol hygroscopic growth and droplet activation observed for hill-capped clouds at connected flow conditions during FEBUKO, Atmos. Environ., 39, 4247–4256, 2005.

Metzger, A., Verheggen, B., Dommen, J., Duplissy, J., Prevot, A. S., Weingartner, E., Riipinen, I., Kulmala, M., Spracklen, D. V., Carslaw, K. S., and Baltensperger, U.: Evidence for the role of organics in aerosol particle formation under atmospheric conditions, P. Natl. Acad. Sci., 107, 6646–6651, doi:10.1073/pnas.0911330107, 2010.

Odedina, M. O.: Rain Attenuation Modeling for Terrestrial & Satellite Communication Services at KU-band and above, Progress report on MSc-thesis, University of Cape Town, 2009.

Otter, L., Guenther, A., Wiedinmyer, C., Fleming, G., Harley, P., and Greenberg, J.: Spatial and temporal variations in biogenic volatile organic compound emissions for Africa south of the equator, J. Geophys. Res., 108, 8505, doi:10.1029/2002JD002609, 2003.

Paasonen, P., Nieminen, T., Asmi, E., Manninen, H. E., Petäjä, T., Plass-Dülmer, C., Flentje, H., Birmili, W., Wiedensohler, A., Hõrrak, U., Metzger, A., Hamed, A., Laaksonen, A., Facchini, M. C., Kerminen, V.-M., and Kulmala, M.: On the roles of sulphuric acid and low-volatility organic vapours in the initial steps of atmospheric new particle formation, Atmos. Chem. Phys., 10, 11223–11242, doi:10.5194/acp-10-11223-2010, 2010.

Petters, M. D. and Kreidenweis, S. M.: A single parameter representation of hygroscopic growth and cloud condensation nucleus activity, Atmos. Chem. Phys., 7, 1961–1971, doi:10.5194/acp-7-1961-2007, 2007.

Petäjä, T., Mauldin III, R. L., Kosciuch, E., McGrath, J., Nieminen, T., Paasonen, P., Boy, M., Adamov, A., Kotiaho, T., and Kulmala, M.: Sulfuric acid and OH concentrations in a boreal forest site, Atmos. Chem. Phys., 9, 7435–7448, doi:10.5194/acp-9-7435-2009, 2009.

Pierce, J. R. and Adams, P. J.: Efficiency of cloud condensation nuclei formation from ultrafine particles, Atmos. Chem. Phys., 7, 1367–1379, doi:10.5194/acp-7-1367-2007, 2007.

Pierce, J. R. and Adams, P. J.: Uncertainty in global CCN concentrations from uncertain aerosol nucleation and primary emission rates, Atmos. Chem. Phys., 9, 1339–1356, doi:10.5194/acp-9-1339-2009, 2009.

Pryor, S. C., Spaulding, A. M., and Barthelmie, R. J.: New particle formation in the Midwwestern USA: Event characteristics, meteorological context and vertical profiles, Atmos. Environ., 44, 4413–4425, 2010.

Qian, S., Sakurai, H., and McMurry, P. H.: Characteristics of regional nucleation events in urban East St. Louis, Atmos. Environ., 41, 4119–4127, 2007.

Quinn, P. K., Bates, T. S., Coffman, D. J., and Covert, D. S.: Influence of particle size and chemistry on the cloud nucleating properties of aerosols, Atmos. Chem. Phys., 8, 1029–1042, doi:10.5194/acp-8-1029-2008, 2008.

Riipinen, I., Pierce, J. R., Yli-Juuti, T., Nieminen, T., Häkkinen, S., Ehn, M., Junninen, H., Lehtipalo, K., Petäjä, T., Slowik, J., Chang, R., Shantz, N. C., Abbatt, J., Leaitch, W. R., Kerminen, V.-M., Worsnop, D. R., Pandis, S. N., Donahue, N. M., and Kulmala, M.: Organic condensation: a vital link connecting aerosol formation to cloud condensation nuclei (CCN) concentrations, Atmos. Chem. Phys., 11, 3865–3878, doi:10.5194/acp-11-3865-2011, 2011.

Rohrer, F. and Berresheim, H.: Strong correlation between levels of tropospheric hydroxyl radicals and solar ultraviolet radiation, Nature, 442, 184–187, doi:10.1038/nature04924, 2006.

Ross, K. E., Piketh, S. J., Bruintjes, R. T., Burger, R. P., Swap, R. J., and Annegarn, H. J.: Spatial and seasonal variations in CCN distribution and the aerosol-CCN relationship over southern Africa, J. Geophys. Res., 108, 8481, doi:10.1029/2002JD002384, 2003.

Schultz, M. G., Heil, A., Hoelzemann, J. J., Spessa, A., Thonicke, K., Goldammer, J. G., Held, A. C., Pereira, J. M. C., and van het Bolscher, M.: Global wildland fire emissions from 1960 to 2000, Global Biogeochem. Cy., 22, GB2002, doi:10.1029/2007GB003031, 2008.

Spracklen, D. V., Pringle, K. J., Carslaw, K. S., Chipperfield, M. P., and Mann, G. W.: A global off-line model of size-resolved aerosol microphysics: I. Model development and prediction of aerosol properties, Atmos. Chem. Phys., 5, 2227–2252, doi:10.5194/acp-5-2227-2005, 2005.

Spracklen, D. V., Carslaw, K. S., Kulmala, M., Kerminen, V.-M., Mann, G. W., and Sihto, S.-L.: The contribution of boundary layer nucleation events to total particle concentrations on regional and global scales, Atmos. Chem. Phys., 6, 5631–5648, doi:10.5194/acp-6-5631-2006, 2006.

Spracklen, D. V., Carslaw, K. S., Kulmala, M., Kerminen, V.-M., Sihto, S.-L., Riipinen, I., Merikanto, J., Mann, G. W., Chipperfield, M. P., Wiedensohler, A., Birmili, W., and Lihavainen, H.: Contribution of particle formation to global cloud condensation nuclei concentrations, Geophys. Res. Lett., 35, L06808, doi:10.1029/2007GL033038, 2008.

Spracklen, D. V., Carslaw, K. S., Merikanto, J., Mann, G. W., Reddington, C. L., Pickering, S., Ogren, J. A., Andrews, E.,

Baltensperger, U., Weingartner, E., Boy, M., Kulmala, M., Laakso, L., Lihavainen, H., Kivekäs, N., Komppula, M., Mihalopoulos, N., Kouvarakis, G., Jennings, S. G., O'Dowd, C., Birmili, W., Wiedensohler, A., Weller, R., Gras, J., Laj, P., Sellegri, K., Bonn, B., Krejci, R., Laaksonen, A., Hamed, A., Minikin, A., Harrison, R. M., Talbot, R., and Sun, J.: Explaining global surface aerosol number concentrations in terms of primary emissions and particle formation, Atmos. Chem. Phys., 10, 4775–4793, doi:10.5194/acp-10-4775-2010, 2010.

Tyson, P. D. and Preston-Whyte, R. A.: The weather and Climate of Southern Africa, Oxford University Press Southern Africa, 2000.

Vakkari, V., Laakso, H., Kulmala, M., Laaksonen, A., Mabaso, D., Molefe, M., Kgabi, N., and Laakso, L.: New particle formation events in semi-clean South African savannah, Atmos. Chem. Phys., 11, 3333–3346, doi:10.5194/acp-11-3333-2011, 2011.

van der Werf, G. R., Randerson, J. T., Giglio, L., Collatz, G. J., Kasibhatla, P. S., and Arellano Jr., A. F.: Interannual variability in global biomass burning emissions from 1997 to 2004, Atmos. Chem. Phys., 6, 3423–3441, doi:10.5194/acp-6-3423-2006, 2006.

Vehkamäki, H., Kulmala, M., Napari, I., Lehtinen, K. E. J., Timmreck, C., Noppel, M., and Laaksonen, A.: An improved parameterization for sulfuric acid-water nucleation rates for tropospheric and stratospheric conditions, J. Geophys. Res.-Atmos., 107, 4622–4631, 2002.

Wang, M. and Penner, J. E.: Aerosol indirect forcing in a global model with particle nucleation, Atmos. Chem. Phys., 9, 239–260, doi:10.5194/acp-9-239-2009, 2009.

Wiedensohler, A., Cheng, Y. F., Nowak, A., Wehner, B., Achtert, P., Berghof, M., Birmili, W., Wu, Z. J., Hu, M., Zhu, T., Takegawa, N., Kita, K., Kondo, Y., Lou, S., Hofzumahaus, A., Holland, F., Wahner, A., Gunthe, S. S., Rose, D., Su, H., and Pöschl, U.: Rapid aerosol particle growth and increase of cloud condensation nucleus activity by secondary aerosol formation and condensation: A case study for regional air pollution in north eastern China, J. Geophys. Res.-Atmos., 114, D00G08, doi:10.1029/2008JD010884, 2009.

Wiedensohler, A., Birmili, W., Nowak, A., Sonntag, A., Weinhold, K., Merkel, M., Wehner, B., Tuch, T., Pfeifer, S., Fiebig, M., Fjäraa, A. M., Asmi, E., Sellegri, K., Depuy, R., Venzac, H., Villani, P., Laj, P., Aalto, P., Ogren, J. A., Swietlicki, E., Williams, P., Roldin, P., Quincey, P., Hüglin, C., Fierz-Schmidhauser, R., Gysel, M., Weingartner, E., Riccobono, F., Santos, S., Grüning, C., Faloon, K., Beddows, D., Harrison, R., Monahan, C., Jennings, S. G., O'Dowd, C. D., Marinoni, A., Horn, H.-G., Keck, L., Jiang, J., Scheckman, J., McMurry, P. H., Deng, Z., Zhao, C. S., Moerman, M., Henzing, B., de Leeuw, G., Löschau, G., and Bastian, S.: Mobility particle size spectrometers: harmonization of technical standards and data structure to facilitate high quality long-term observations of atmospheric particle number size distributions, Atmos. Meas. Tech., 5, 657–685, doi:10.5194/amt-5-657-2012, 2012.

Winklmayr, W., Reischl, G., Lindner, A., and Berner, A.: A new electromobility spectrometer for the measurement of aerosol size distributions in the size range from 1 to 1000 nm, J. Aerosol Sci., 22, 289–296, 1991.

Yli-Juuti, T., Nieminen, T., Hirsikko, A., Aalto, P. P., Asmi, E., Hõrrak, U., Manninen, H. E., Patokoski, J., Dal Maso, M., Petäjä, T., Rinne, J., Kulmala, M., and Riipinen, I.: Growth rates of nucleation mode particles in Hyytiälä during 2003–2009: variation with particle size, season, data analysis method and ambient conditions, Atmos. Chem. Phys., 11, 12865–12886, doi:10.5194/acp-11-12865-2011, 2011.

Yu, F.: A secondary organic aerosol formation model considering successive oxidation aging and kinetic condensation of organic compounds: global scale implications, Atmos. Chem. Phys., 11, 1083–1099, doi:10.5194/acp-11-1083-2011, 2011.

Yu, F. and Luo, G.: Simulation of particle size distribution with a global aerosol model: contribution of nucleation to aerosol and CCN number concentrations, Atmos. Chem. Phys., 9, 7691–7710, doi:10.5194/acp-9-7691-2009, 2009.

Zhou, J.: Hygroscopic properties of atmospheric aerosol particles in various environments, Ph.D. thesis, University of Lund, Division of Nuclear Physics, Sweden, 2001.